X-irradiation induces cell death in fetal fibroblasts

MICHAËL BECK[1,2], MARJAN MOREELS[1], PAUL JACQUET[1], PATRICK VAN OOSTVELDT[2,3],
WINNOK H. DE VOS[2,3] and SARAH BAATOUT[1,2]

[1]Laboratory of Molecular and Cellular Biology, Institute for Environment, Health and Safety, Belgian Nuclear Research Centre,
SCK•CEN, Mol; [2]Department of Molecular Biotechnology, [3]NB-photonics, Ghent University, Ghent, Belgium

Abstract. The impact of ionizing radiation on developing organisms has been widely studied for risk assessment purposes. Even though efforts have been made to decrease received doses to as low as reasonably achievable, the possibility of accidental exposure has to be considered as well. Mammalian gestation is usually divided into three periods. Radiation exposure during the 'pre-implantation period' may essentially result in embryonic mortality while exposure during the 'organogenesis period' may characteristically lead to malformations. In humans, the 'fetal period' is one of particular sensitivity to radiation induction of mental retardation, especially if the exposure occurs between weeks 8-15 of gestation. It is also admitted that prenatal irradiation may increase the risk of leukemia and childhood cancer, with an equal risk over the whole pregnancy. The aim of this study was to investigate the effects of moderate to high doses of X-irradiation on mouse skin fetal fibroblasts, one of the cell types subjected to the highest dose of radiation. Exposure of the cells to X-rays led to a rapid and significant increase in γ-H2AX foci, indicative of high levels of DNA double strand breaks. High doses (>2 Gy) also led to a pronounced G2-arrest and a decrease in the number of cells in the S phase, which was followed after 24 h by a decrease in cell survival and an increase in the level of apoptosis and necrosis. This study shows that mouse fetal skin fibroblasts are sensitive to high doses of X-irradiation. Furthermore, we report a better repair for higher doses than lower, which seems to indicate that little DNA damage is not necessarily repaired immediately. However, more sensitive approaches are necessary to identify the risk associated with low doses of radiation.

Introduction

Among the somatic effects of radiation other than cancer, developmental effects on the unborn child are of greatest concern. The principal factors of importance for the induction of developmental effects are the dose and the stage of gestation at which it is delivered. In this view, embryonic development may be divided into three periods, each of them showing a characteristic sensitivity to ionizing radiation and other external agents (1,2). Thus, lethality has been recognized as the main effect of irradiation during the pre-implantation period (weeks 0-2 of pregnancy) while in the organogenesis period (weeks 2-8), the main effect of radiation will consist in the production of a variety of malformations. Embryos exposed during the organogenesis period may also show growth retardation expressed as a weight reduction at term. The consequences of an exposure of mammalian embryos to ionizing radiation during the fetal period (8th week to delivery) may include tissue anomalies and growth retardation which frequently persists during all the extra-uterine life. Other effects may include fertility changes or effects on the hematopoietic system, liver and kidney, which occur after fairly high radiation doses (3). In humans, the fetal period is also one of particular sensitivity to radiation induction of mental retardation, especially if the exposure occurs during weeks 8-15 (4). A further potential effect of prenatal irradiation is an increase of the risk of leukaemia and childhood cancer, with a relative risk recently estimated at 1.4 (i.e., a 40% increase over the background risk which is 0.2-0.3%) following a fetal dose of approximately 10 mGy (5). This risk is assumed to be the same for all three periods of embryonic development.

At the cellular level, DNA double strand breaks (DSB) are assumed to constitute the major radiation-induced cytotoxic lesions. Improperly repaired DSB may result in DNA sequence integrity alterations or to cell death (6-11). While excessive cell death may lead to embryonic malformations and growth retardation, persisting alterations in DNA may be transmitted to the daughter cells of the embryos thereby increasing the risk for postnatal cancer or genetic diseases.

In the present study, we investigated the impact of X-irradiation on a skin fibroblast cell line originating from mouse fetuses (STO). Cells were exposed to increasing doses of X-irradiation and DNA damage and other biological end-points (cellular morphology, proliferation, cell cycle and cell death) were measured at different times after irradiation.

Materials and methods

Cell culture and X-irradiation. The STO [SIM (Sandos inbred mice) thioguanine- and ouabain-resistant] cell line is derived

---

Correspondence to: Professor Sarah Baatout, Laboratory of Molecular and Cellular Biology, Institute for Environment, Health and Safety, Belgian Nuclear Research Centre (SCK•CEN), Boeretang 200, B-2400 Mol, Belgium
E-mail: sarah.baatout@sckcen.be

from a continuous line of SIM skin fibroblasts (12,13). STO cells were cultured in DMEM (Invitrogen NV/SA, Belgium) supplemented with 10% fetal bovine serum (FBS, Invitrogen NV/SA) and 1% penicillin/streptomycin (Invitrogen NV/SA). Cells (6 ml) at a density of $1x10^5$ cells/ml (or $2x10^5$, for γ-H2AX assessment only) were seeded in 25 cm^2 tissue culture flasks and placed in a humidified incubator (37˚C; 5% CO_2). Twenty-four hours after plating, medium was replaced and cells were irradiated with the following doses of X-irradiation: 0, 0.25, 0.5, 1, 2 or 4 Gy (250 keV, 15 mA, 1 mm Cu). The dose rate was 0.273±0.006 Gy/min and the accuracy of the given dose was higher than 99.99%. Cells were washed 30 min, 120 min or 24 h after irradiation with phosphate buffered saline (PBS, Invitrogen NV/SA) and detached by trypsin-EDTA (0.05%) (Invitrogen NV/SA). After 5 min, trypsin was inhibited with FBS and cells were treated according to the following protocols.

Flow cytometry. Cell size, cell cycle, absolute cell counts, Annexin V/propidium iodide (PI), caspase-3 activity and γ-H2AX were measured using a Beckman Coulter EPICS XL flow cytometer. For all assays, at least 10,000 cells were analyzed in triplicates for each condition.

DNA double strand breaks (γ-H2AX). Cells were collected and processed either 30 or 120 min after irradiation following the manufacturer's instructions of the kit H2AX phosphorylation/DNA damage assay (Millipore, Brussels, Belgium). The samples were then analyzed by flow cytometry.

Cell cycle analysis. Twenty-four hours after X-irradiation, cells were fixed in cold ethanol (80%). After a fixation of at least 1 h, cells were washed in PBS and suspended in a solution of PI (Sigma-Aldrich NV/SA, Belgium) containing RNAse (10 mM Tris, 5 mM $MgCl_2$, 10 μg/ml RNAse, 40 μg/ml PI) before being incubated at 37˚C for 1 h. Estimation of G1, S and G2 fractions was performed by flow cytometry after discrimination of doublets and aggregates using red fluorescence pulse width analysis. In addition to gating away doublets and aggregates, signals from cells with less than half the DNA content of G1 cells were excluded to avoid micronuclei and apoptotic bodies. The mitotic index (MI) was calculated as followed: MI = [(1xG1)+(1.5xS)+(2xG2)]/100.

Absolute cell count and size assessments. To measure the absolute cell count, all the cells (adherent and floating) were collected 24 h after irradiation, and 50 μl of beads (Flow-Count™, Beckman Coulter, Fullerton, CA, USA) were added to 950 μl of each sample and measured by flow cytometry according to the manufacturer's instructions. The absolute number of cells was calculated as followed: (c/b)*d where c is the counted number of cells for 1,000 beads, b is the volume containing 1,000 beads in the sample (20.70 μl) and d is the total volume collected (2,500 μl).

The absolute diameter of the cells (in μm) was calculated using the Flow Cytometry Size Calibration kit according to the manufacturer's instructions (Molecular Probes, Eugene, OR, USA).

Cell morphology. Twenty-four hours after X-irradiation, cells were detached by trypsin-EDTA 0.05%, washed twice in PBS
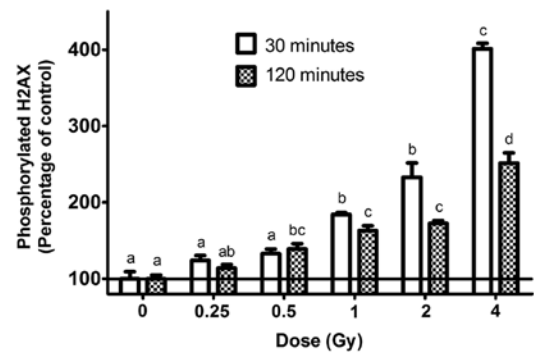

Figure 1. Histogram of γ-H2AX quantification by flow cytometry of STO cells 30 and 120 min after X-irradiation. The vertical axis represents γ-H2AX intensity as a percentage of controls (mean ± SEM). Data were analyzed by two-way ANOVA and means separated per time-point (in groups a-d) by a Sidak *post ho*c test.

supplemented with 10% FBS and suspended in 1 ml of PBS supplemented with 1% FBS. Next, cells were centrifuged onto a slide by cytospinning at 500 rpm for 5 min. The slides were finally stained with May-Grünwald Giemsa. Light microscopy was used to detect the number of abnormal cells. Cells (n=100) were counted from each of the 3 biological replicates prepared for each dose and scored for normality, vacuoles and morphological signs of apoptosis (cell blebs).

Apoptosis (Annexin V/PI, caspase-3 activity and sub-G1 peak). Twenty-four hours after irradiation, cells were processed following the manufacturer's instructions of the Annexin V-FITC Kit (Bender MedSystems Diagnostics GmbH, Vienna, Austria) to assess phosphatidylserine asymmetry, characteristic of apoptotic cells, or cells with disrupted membrane, characteristic of necrotic cells (14). Annexin V-positive/PI-negative cells were considered as apoptotic, double-positive cells as necrotic, double-negative as living cells and Annexin V-negative/PI-positive cells were considered as damaged.

Caspase-3 activity assessment was performed following the manufacturer's instructions of the CaspGlow™ kit (Medical and Biological Laboratories Co., Ltd., Woburn, MA, USA).

While performing cell cycle analysis, cells that showed a red fluorescence corresponding to a DNA content included between half the mean channel of G1 phase and G1 phase were referred as sub-G1 cells.

Statistical analyses. Graphics were performed with Graph Pad Prism version 5.00 (GraphPad Software Inc., USA), while statistics were performed with SPSS version 17.0 (IBM Corp., USA). Kolmogorov-Smirnov test was achieved to verify that the data were parametric and Sidak *post hoc* test was used to analyze differences between treatments. All data were tested for homogeneity of variance before one-way and two-way ANOVA analysis. Differences between means were considered significant for p-values <0.05.

Results

DNA double strand breaks. We report a significant dose-dependent increase of γ-H2AX (Fig. 1) as measured by flow cytometry, which reached 400% compared to controls, 30 min
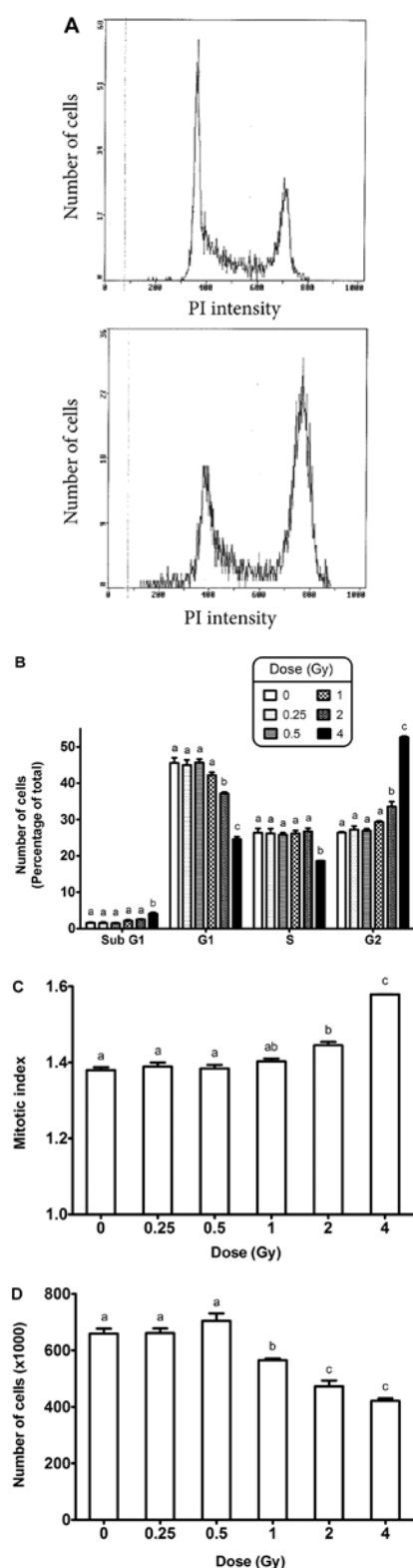
Figure 2. Cell cycle alterations of STO cells 24 h after X-irradiation. (A) Representative cell cycle distributions performed by flow cytometry analysis after propidium iodide staining of controls (top) and 4 Gy irradiated cells (below). A cell cycle arrest was observed in G2 phase along with an increase of sub-G1 peak. (B) Quantitative analysis of cell cycles measured by flow cytometry (mean ± SEM). A significant (one-way ANOVA) increase of cells in G2 phase along with a decrease of cells in G1 and S phase were observed. Data were analyzed by one-way ANOVA and means separated per cell cycle phase (in groups a-d) by a Sidak *post hoc* test. (C) Mitotic indexes calculated from the cell cycle (mean ± SEM). The mitotic index was shown to significantly increase in a dose-dependent manner (one-way ANOVA, Sidak *post hoc* test). (D) Absolute number of cells counted by flow cytometry (mean ± SEM). A significantly lower amount of cells (one-way ANOVA, Sidak *post hoc* test) indicates reduced proliferation and increased cell death.

after exposure to 4 Gy. After 120 min, γ-H2AX levels decreased compared to 30 min, especially for high doses (1, 2 and 4 Gy). Two-way ANOVA analysis showed a significant effect of time, dose and interaction of both factors.

Cell cycle and proliferation. Fig. 2A shows representative histograms of the cell cycle of STO cells 24 h after X-irradiation (4 Gy) compared to control conditions, measured by flow cytometry. A shift between the proportion of cells within the G1 and the G2/M phases is observed (Fig. 2B), with the presence of a significant increase in the number of cells in G2 phase (>2 Gy). The mitotic index (Fig. 2C) significantly increased at higher doses (2 and 4 Gy), as calculated from the proportion cells in each phase. These effects were proportionally and linearly correlated with the dose of X-rays.

We also observed a significant dose-dependent decrease in the number of cells after X-irradiation (Fig. 2D). However, no significant effect was observed for medium doses (0.25 and 0.5 Gy), but only in high doses (1, 2 and 4 Gy).

Morphological alterations. Dose-dependent increases in the number of cells with morphological characteristics of apoptosis (blebs) and with vacuoles were observed by microscopy 24 h after irradiation (Fig. 3A and B). The increase in the number of apoptotic cells was significant starting from a dose of 0.5 Gy. Besides apoptosis, we observed polynuclei and DNA fragmentation by microscopy at 4 Gy (data not shown) and flow cytometry analysis revealed a significant increase in cell size when STO cells were exposed to doses ranging from 1 to 4 Gy of X-rays (Fig. 3C).

Apoptosis and necrosis. Significant increases in apoptotic as well as of necrotic cells were observed by flow cytometry, accompanied by a decrease of living cells correlated to the radiation dose. This dose-dependent increase was significant upon exposure to 1 Gy of X-rays onwards. At 4 Gy, 20% of the cells were counted as apoptotic and 17% were counted as necrotic (Fig. 4A), confirming that at high doses of X-rays, apoptosis and necrosis play a significant role in cell death.

Moreover, a significant increase from 2 Gy onwards of the pro-apoptotic caspase-3 activity was measured by flow cytometry (Fig. 4B), reaching 200% at 4 Gy. From the cell cycle analysis, a sub-G1 peak was detected at the highest dose (4 Gy) (Fig. 2B).

Discussion

It is well known that ionizing radiation induces a large spectrum of DNA lesions including double strand breaks (DSB) (11). The global response of a cell to DNA damage is an extremely complex scheme that triggers multiple pathways involved in sensing DNA damage, activating cell cycle check-points and inducing DNA repair (15). DNA damage response leads to three possible cell fates, including survival, apoptosis when the cell is incapable of repairing, or altered survival in case of incorrect repair leading to possible genomic instability (16).

H2AX is a modified histone that is phosphorylated by ataxia telangiectasia mutated (ATM), ataxia telangiectasia and Rad3-related (ATR) or DNA-dependent protein kinase catalytic subunit (DNA-PK) as a DSB is induced. It facilitates DNA repair
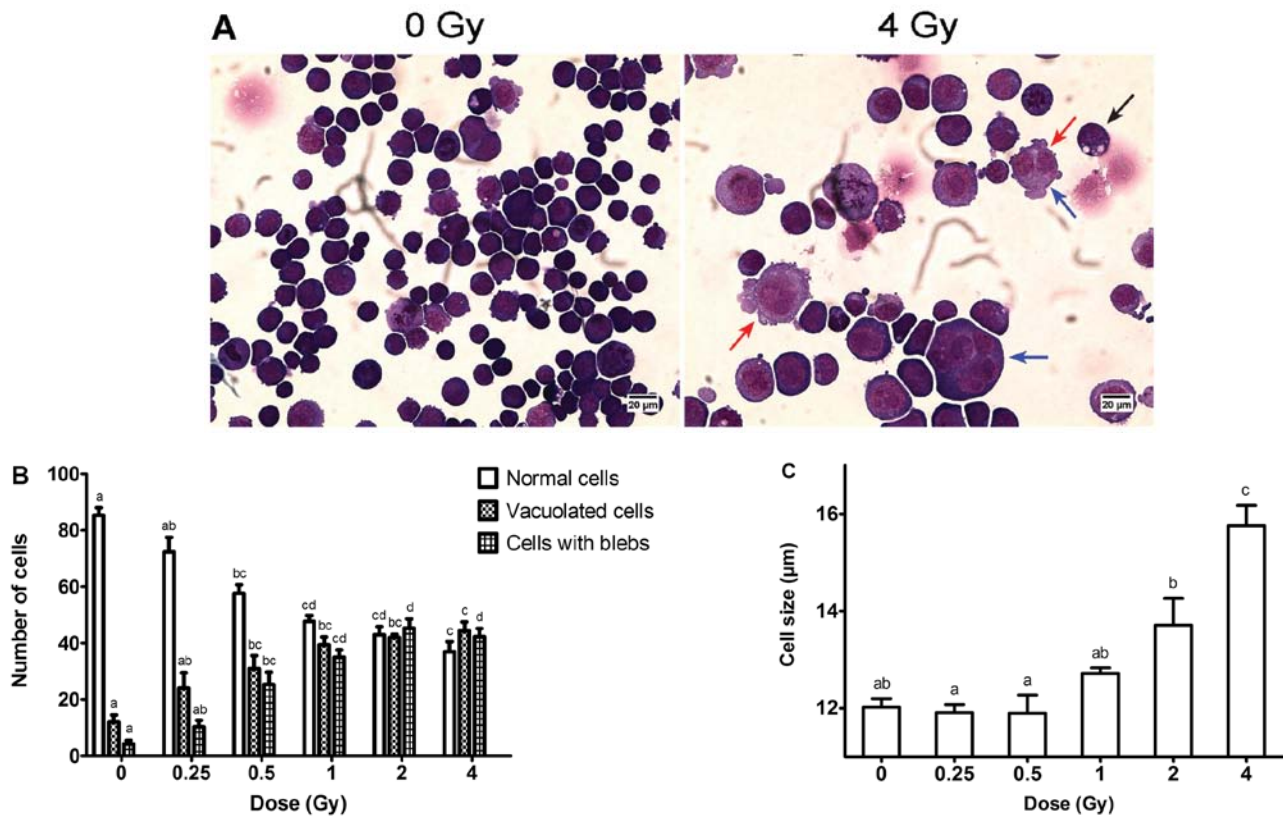
Figure 3. Morphological alterations of STO cells 24 h after X-irradiation. (A) Representative pictures of May-Grünwald Giemsa stained slides performed on cytospinned cells. Controls are shown on the left and 4 Gy irradiated are shown on the right. Arrows show examples of cells with blebs (red), vacuoles (black) or polynuclei (blue). (B) Histogram of the number (mean ± SEM) of normal, vacuolated and apoptotic (blebs) cells, counted from May-Grünwald Giemsa stained slides. Data were analyzed by one-way ANOVA and means separated per type (in groups a-d) by a Sidak *post hoc* test. (C) Histogram of the dose-dependent cell size increase (mean ± SEM) measured by flow cytometry (one-way ANOVA, Sidak *post hoc* test).
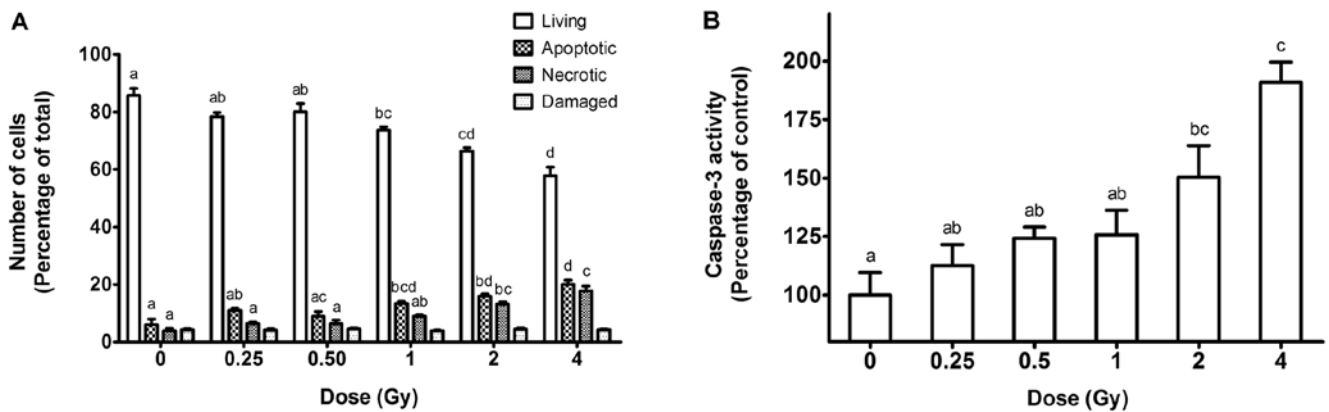

Figure 4. Apoptotic and necrotic status of STO cells 24 h after X-irradiation. (A) Histogram of the number of living, apoptotic, necrotic and damaged cells measured by Annexin V/PI assay (mean ± SEM). Significant decrease of living cells and increases of apoptotic and necrotic cells reaching, respectively, 20 and 17% of the total cell population upon a dose of 4 Gy were observed. Data were analyzed by one-way ANOVA and means separated per phenotype (in groups a-d) by a Sidak *post hoc* test. (B) Histogram of caspase-3 activity, an effector protein of apoptosis, measured by flow cytometry (mean ± SEM). A significant dose-dependent increase of caspase-3 activity was observed.

possibly by chromatin reorganization (17) and/or by recruiting and activating repair factors such as ATM (17,18). Besides their biological role in DNA damage response, γ-H2AX foci are used as a marker of radiation-induced DSB (17,19,20). Phosphorylation of H2AX is a fast process, as the maximal value is reached between 9 and 30 min (19). The amount of γ-H2AX that we measured 30 min after irradiation was significant (>1 Gy). These levels decreased in time, as we showed that γ-H2AX reached about 0.6 times the signal 120 min after radiation for the highest dose (4 Gy). However, for doses lower than 1 Gy, no significant loss of γ-H2AX was detected, suggesting that the more a cell is damaged, the more effective it is in repairing this DNA damage. This might be explained by the fact that, upon exposure of STO cells to X-irradiation, most of the DNA damage is repaired

quickly by non-homologous end joining repair (NHEJ) (8). Remaining errors would lead to a G2 cell cycle arrest, where homologous recombination (HR) plays a role in repairing and correcting errors left by the error prone NHEJ. Indeed, HR operates only in the S/G2 phase, since it needs accessible homologous chromatin regions (21) and the activation of cyclin-dependent kinases, down regulated in G1 phase, is required for HR (11). Moreover, a small number of errors does not seem to be necessarily repaired immediately and the presence of γ-H2AX foci is bound to stay until further repair (error corrections) (9).

Our hypothesis, confirmed by flow cytometry, is that radiation-induced DNA damage triggers cell cycle arrest in G2 phase, thereby inhibiting cell proliferation and promoting DNA repair (7,8,22). These results are consistent with a recent similar study performed on murine osteoblasts (23). Moreover, cell cycle arrest has already been shown in fibroblasts with the same range of X-ray dose (24). In G2 phase, cells are larger in size, as measured by flow cytometry. High doses of X-rays induced a decrease in the absolute number of cells, indicating a decrease of cell proliferation and/or an increase of cell death. As far as cell survival is concerned, May-Grünwald Giemsa staining performed 24 h after irradiation showed that mouse fetal fibroblasts exhibited significant morphological signs of cell damage by X-rays from lower (0.5 Gy) to higher doses and that exposure to 1-4 Gy leads to an increased apoptotic phenotype. Moreover, by measuring the activity of an important apoptotic actor, caspase-3, and the loss of phosphatidylserine asymmetry, another characteristic of an apoptotic phenotype, we showed that apoptosis plays a role in radiation-induced cell death at doses of 1-4 Gy of X-rays. Furthermore, an increase of sub-G1 cells was detected by flow cytometry on a cell cycle analysis and a significant increase in cellular blebs was observed by microscopy, starting from 0.5 Gy.

In conclusion, we show that high doses of X-irradiation induce DSB leading to a G2 cell cycle arrest and increased cell death by apoptosis and necrosis in fetal skin fibroblasts. At the highest doses, DSB measured by γ-H2AX decreased quickly in time. However, a low level of γ-H2AX remained, comparable to the level reached with medium doses, probably to allow time for further repair. Although our study shows that mouse fetal skin fibroblasts are sensitive to high doses of X-irradiation, response to low doses of radiation remains poorly understood. Therefore, more research in cellular response mechanisms of developing organisms is important for radiation risk assessment.

Acknowledgements

References

1. Jacquet P: Sensitivity of germ cells and embryos to ionizing radiation. J Biol Regul Homeost Agents 18: 106-114, 2004.
2. UNSCEAR: Report to the General Assembly with Annexes. United Nations Scientific Committee on the Effects of Atomic Radiation (UNSCEAR), New York, 1986.
3. Hall EJ: Radiobiology for the Radiologist. Lippincott Williams & Wilkins, 1988.
4. Otake M, Schull WJ and Lee S: Threshold for radiation-related severe mental retardation in prenatally exposed A-bomb survivors: a re-analysis. Int J Radiat Biol 70: 755-763, 1996.
5. ICRP: Pregnancy and medical radiation. ICRP Publication 84. In: Annals of the ICRP, 2000.
6. Costes SV, Boissiere A, Ravani S, Romano R, Parvin B and Barcellos-Hoff MH: Imaging features that discriminate between foci induced by high- and low-LET radiation in human fibroblasts. Radiat Res 165: 505-515, 2006.
7. Belli M, Sapora O and Tabocchini MA: Molecular targets in cellular response to ionizing radiation and implications in space radiation protection. J Radiat Res (Tokyo) 43 (Suppl): S13-S19, 2002.
8. Stenerlöw B, Ekerljung L, Carlsson J and Lennartsson J: Radiation induced DNA-damage/repair and associated signaling pathways. In: Targeted Radionuclide Tumor Therapy. Stigbrand T, Carlsson J and Adams GP (eds.) Springer Science, pp249-266, 2008.
9. Olive PL and Banath JP: Phosphorylation of histone H2AX as a measure of radiosensitivity. Int J Radiat Oncol Biol Phys 58: 331-335, 2004.
10. Radford IR: The level of induced DNA double-strand breakage correlates with cell killing after X-irradiation. Int J Radiat Biol Relat Stud Phys Chem Med 48: 45-54, 1985.
11. Jeggo P and Lavin MF: Cellular radiosensitivity: how much better do we understand it? Int J Radiat Biol 85: 1061-1081, 2009.
12. Ware LM and Axelrad AA: Inherited resistance to N- and B-tropic murine leukemia viruses in vitro: evidence that congenic mouse strains SIM and SIM.R differ at the Fv-1 locus. Virology 50: 339-348, 1972.
13. Koch KS, Son KH, Maehr R, et al: Immune-privileged embryonic Swiss mouse STO and STO cell-derived progenitor cells: major histocompatibility complex and cell differentiation antigen expression patterns resemble those of human embryonic stem cell lines. Immunology 119: 98-115, 2006.
14. Wilson GD and Marples B: Flow cytometry in radiation research: past, present and future. Radiat Res 168: 391-403, 2007.
15. Su TT: Cellular responses to DNA damage: one signal, multiple choices. Annu Rev Genet 40: 187-208, 2006.
16. Verheij M and Bartelink H: Radiation-induced apoptosis. Cell Tissue Res 301: 133-142, 2000.
17. Fernandez-Capetillo O, Lee A, Nussenzweig M and Nussenzweig A: H2AX: the histone guardian of the genome. DNA Repair (Amst) 3: 959-967, 2004.
18. Kobayashi J, Tauchi H, Chen B, et al: Histone H2AX participates the DNA damage-induced ATM activation through interaction with NBS1. Biochem Biophys Res Commun 380: 752-757, 2009.
19. Rogakou EP, Pilch DR, Orr AH, Ivanova VS and Bonner WM: DNA double-stranded breaks induce histone H2AX phosphorylation on serine 139. J Biol Chem 273: 5858-5868, 1998.
20. Kinner A, Wu W, Staudt C and Iliakis G: Gamma-H2AX in recognition and signaling of DNA double-strand breaks in the context of chromatin. Nucleic Acids Res 36: 5678-5694, 2008.
21. Bassing CH and Alt FW: The cellular response to general and programmed DNA double strand breaks. DNA Repair (Amst) 3: 781-796, 2004.
22. Schmitt E, Paquet C, Beauchemin M and Bertrand R: DNA-damage response network at the crossroads of cell-cycle checkpoints, cellular senescence and apoptosis. J Zhejiang Univ Sci B 8: 377-397, 2007.
23. Lau P, Baumstark-Khan C, Hellweg CE and Reitz G: X-irradiation-induced cell cycle delay and DNA double-strand breaks in the murine osteoblastic cell line OCT-1. Radiat Environ Biophys 49: 271-280, 2010.
24. Nasonova E, Fussel K, Berger S, Gudowska-Nowak E and Ritter S: Cell cycle arrest and aberration yield in normal human fibroblasts. I. Effects of X-rays and 195 MeV u(-1) C ions. Int J Radiat Biol 80: 621-634, 2004.